PAPER

(TeCl)$_4$(TiCl$_4$) with isolated Te$_4$Cl$_{16}$ and TiCl$_4$ molecules and second-harmonic-generation†

Maxime A. Bonnin,[a] Klaus Beier,[a] Lkhamsuren Bayarjargal, [iD][b] Björn Winkler [iD] *[b] and Claus Feldmann [iD] *[a]

(TeCl$_4$)$_4$(TiCl$_4$) is obtained by reaction of TeCl$_4$ and TiCl$_4$ at 50 °C with quantitative yield. The compound is composed of isolated, molecular (TeCl$_4$)$_4$ heterocubane-type units as well as isolated, molecular TiCl$_4$ tetrahedra. The (TeCl$_4$)$_4$ heterocubane is arranged like a body-centred cubic cell with TiCl$_4$ tetrahedra occupying 4 of 6 octahedral sites. (TeCl$_4$)$_4$(TiCl$_4$) crystallizes in the space group $I\bar{4}$ with an unidirectional alignment of the tetrahedral building units. The structure of the compound is obtained from single crystal X-ray diffraction and confirmed by Rietveld refinement of powder diffraction data. Thermogravimetry, optical spectroscopy, infrared and Raman spectroscopy are employed to further characterize the title compound. Second harmonic generation (SHG) is observed with a strong intensity (1.6-times higher than potassium dihydrogen phosphate/KDP). The SHG effect is observed in the visible spectral regime as the band gap, derived from a Tauc plot, is 2.8 eV.

Introduction

Crystalline solid compounds composed of tetrahedral building units often show interesting material features such as non-linear optical (NLO) properties.[1] Quartz with (SiO$_4$) tetrahedra is a well-known example showing piezoelectricity, circular dichroism and second harmonic generation (SHG).[2] In particular, SHG materials are highly relevant for application and are widely used for frequency doubling of lasers (*e.g.*, Nd:YAG: 1064 nm → 532 nm; Ti:sapphire: 800 nm → 400 nm).[3] A key requirement for NLO properties is the absence of inversion symmetry, which – for tetrahedral arrangements – can occur due to an unidirectional orientation of the tetrahedral building units. While the SHG intensity is comparably weak in quartz, potassium dihydrogen phosphate (KDP) containing [H$_2$PO$_4$]$^-$ tetrahedra is known for its very strong SHG effect.[4] Other examples include materials like iodates (*e.g.* Li$_2$Ge(IO$_3$)$_6$), selenites (*e.g.* Bi$_3$(SeO$_3$)$_3$(Se$_2$O$_5$)F), or tellurites (Ba(MoO$_2$F)$_2$(TeO$_3$)$_2$) with pseudo-tetrahedral [IO$_3$]$^-$, [SeO$_3$]$^{2-}$, or [TeO$_3$]$^{2-}$ units.[5] Beside the absence of inversion symmetry, further material properties determine the intensity of SHG signals and the usefulness of a compound for application.

These include the magnitude of the band gap, whether phase matching is possible, the thermal stability, and a high damage threshold when irradiated with high-intensity laser light.[6]

In principle, tetrahedral arrangements can be easily realized by Lewis-acid–base reactions such as MX$_3$ + M′X$_4$ → [M′X$_3$]$^+$[MX$_4$]$^-$ with a halogen transfer from M′ to M (M: element, M′: element with lone electron pair, X: halogen). Following such synthesis routes, several compounds have already been prepared. In many cases, however, the Lewis-acid–base reaction resulted in compounds crystallizing in space groups with inversion symmetry.[7] Often inversion symmetry is observed if octahedral building units are formed in addition to a tetra-hedral/pseudotetrahedral building unit (*e.g.* [SeCl$_3$][SbCl$_6$], [TeCl$_3$][NbCl$_6$]).[8] Other compounds also crystallize in space groups without inversion symmetry, but potential NLO effects were not examined. Tetrahedral arrangements obtained *via* Lewis-acid–base reactions often offer several advantages such as: (i) simple synthesis with quantitative yield, (ii) straight-forward crystallization and crystal growth, and (iii) a band gap (E_g) at the upper energy edge of the visible spectrum (3.5 eV ≥ E_g ≥ 2.5 eV). Based on the aforementioned considerations, we recently prepared compounds such as [SeCl$_3$]$^+$[GaCl$_4$]$^-$, [TeCl$_3$]$^+$[GaCl$_4$]$^-$,[9] or the molecular Cl$_3$SeOGaCl$_3$,[10] which show promising SHG intensities up to 10× KDP.

Aiming at a realization of novel tetrahedral arrangements with potential SHG effects *via* Lewis-acid–base reactions, here, we explored the reaction of TeCl$_4$ and TiCl$_4$. TeCl$_4$ was expected to serve as a Lewis base and TiCl$_4$ as a Lewis acid, hence leading to a formation of [TeCl$_3$]$^+$[TiCl$_5$]$^-$ or [TeCl$_3$]$_2^+$[TiCl$_6$]$^{2-}$. In contrast to our expectation, (TeCl$_4$)$_4$(TiCl$_4$) was obtained

[a]Institute for Inorganic Chemistry (IAC), Karlsruhe Institute of Technology (KIT), Engesserstraße 15, D-76131 Karlsruhe, Germany. E-mail: claus.feldmann@kit.edu
[b]Institute of Geosciences, Goethe University Frankfurt, Altenhöferallee 1, D-60438 Frankfurt a. M., Germany. E-mail: b.winkler@kristall.uni-frankfurt.de
†Electronic supplementary information (ESI) available. CCDC 2328371. For ESI and crystallographic data in CIF or other electronic format see DOI: https://doi.org/10.1039/d4dt00284a

with isolated molecular, heterocubane-type $(TeCl_4)_4$ tetramers as well as isolated molecular $TiCl_4$ tetrahedra. $(TeCl_4)_4(TiCl_4)$ nevertheless crystallizes without inversion symmetry and shows a strong SHG effect with an intensity of about 1.6× KDP.

Results and discussion

Synthesis

$(TeCl_4)_4(TiCl_4)$ was prepared by reaction of $TeCl_4$ and $TiCl_4$ at 50 °C (Fig. 1). Here, the liquid $TiCl_4$ also serves as the solvent (melting point $TiCl_4$: −24 °C). After one week, colourless transparent crystals were obtained with quantitative yield. In contrast to our expectation, $(TeCl_4)_4(TiCl_4)$ was formed instead of the expected Lewis-acid–base adducts, such as $[TeCl_3]^+[TiCl_5]^-$ or $[TeCl_3]_2^+[TiCl_6]^{2-}$. Although the anion $[TiCl_6]^{2-}$ is well-known (*e.g.* $[NH_4]_2[TiCl_6]$, $Cs_2[TiCl_6]$),[11] sixfold coordination of Ti^{4+} by Cl^- is obviously not preferred at our synthesis conditions and the Lewis acidity of $TiCl_4$ is not high enough for Cl^- subtraction from $TeCl_4$. The grey colour of the product is noteworthy (Fig. 1). It originates from a small amount of elemental tellurium contained as an impurity in the as-supplied $TiCl_4$. The purity of crystals of the title compound was validated by X-ray powder diffraction (XRD) with a Rietveld refinement of the diffraction data (Fig. 2), Fourier-transform infrared (FT-IR) spectroscopy, and thermogravimetry (TG) (see below). $(TeCl_4)_4(TiCl_4)$ is very sensitive to moisture and needs to be handled and stored under inert conditions.

Structural characterization

According to X-ray structure analysis based on single crystals, $(TeCl_4)_4(TiCl_4)$ crystallizes in the non-centrosymmetric, tetragonal space group $I\bar{4}$ and consists of isolated, molecular $(TeCl_4)_4$ heterocubane-type units (Fig. 3a; ESI: Table S1, Fig. S1†) and isolated, molecular $TiCl_4$ tetrahedra (Fig. 3b). X-ray powder diffraction with Rietveld refinement was used to confirm the crystal structure and space-group symmetry obtained by single-crystal structure analysis (Fig. 2; ESI: Table S2†). The absence of any center of inversion is clearly reflected by the uniformly oriented tetrahedral and heterocubane-type building units (Fig. 3c). The three-dimensional packing of the $(TeCl_4)_4$ heterocubanes and the $TiCl_4$ tetrahedra can be illustrated by a reduced representation showing only the center of the respective building unit, *i.e.* only the center of
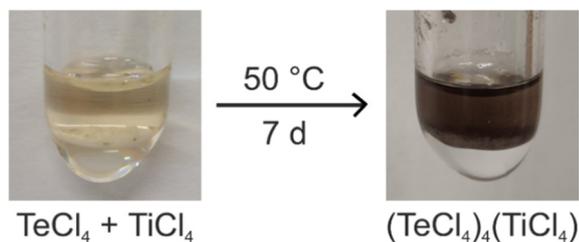

Fig. 1 Scheme illustrating the synthesis of $(TeCl_4)_4(TiCl_4)$ (greyish colour of product due to small amounts of elemental tellurium).
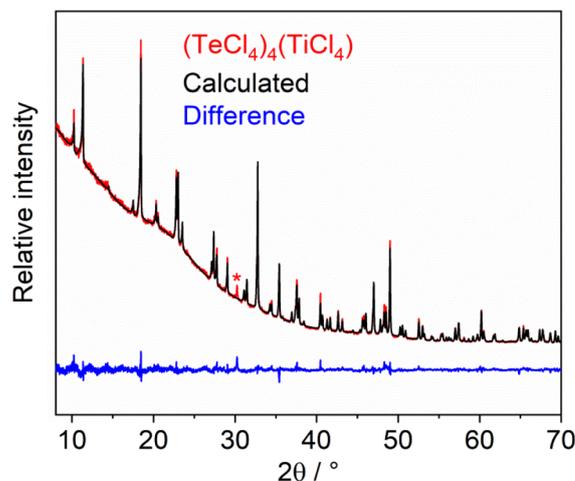

Fig. 2 X-ray powder diffraction of $(TeCl_4)_4(TiCl_4)$ with Rietveld refinement using the data from single-crystal structure analysis as a model: experimental powder diffractogram (red), Rietveld refinement (black), and difference curve (blue) (*single Bragg reflection of elemental tellurium).

the $(TeCl_4)_4$ heterocubane and only Ti for $TiCl_4$ (ESI: Fig. S2†). Such a representation shows that the $(TeCl_4)_4$ heterocubane serves as packing unit of a body-centred cubic (bcc) cell. In this bcc cell, the $TiCl_4$ tetrahedra occupy 4 of 6 octahedral sites.

Both molecular units in $(TeCl_4)_4(TiCl_4)$ – $(TeCl_4)_4$ heterocubanes and $TiCl_4$ tetrahedra – retain structural similarities to the respective starting materials. Thus, the $(TeCl_4)_4$ heterocubane exhibits four edge-sharing $(TeCl_6)$ octahedra with Te–Cl distances (231.2(2)–295.4(1) pm) and Cl–Te–Cl angles (84.2(1)–95.0(1)°) similar to $TeCl_4$ (Te–Cl: 229.6–295.9 pm, Cl–Te–Cl: 84.0–95.7°).[12] Te–Cl distances with terminal Cl (231.2(2)–231.9(1) pm) are as expected significantly shorter than distances involving bridging Cl ligands (289.0(1)–295.4(1) pm). The Cl–Te–Cl angles indicate the slightly distorted octahedral coordination. The Ti–Cl distances (216.4(2) pm) and Cl–Ti–Cl angles (108.7(1)–109.9(1)°) are similar to $TiCl_4$ (Ti–Cl: 216.3–216.5 pm, Cl–Ti–Cl: 108.9–109.9°).[13] A mixed molecular compound and co-crystallization of $TeCl_4$ and $TiCl_4$, to the best of our knowledge, is observed here for the first time. An isolated $(TeCl_4)_4$ tetramer was not observed in a compound until now (except for pure $TeCl_4$ itself). In addition, only anionic units such as $[Te_4Cl_{18}]^{2-}$ were reported before.[14] Moreover, isolated molecular $TiCl_4$ tetrahedra without further ligands were up to now only reported in combination with fullerenes (*e.g.* $C_{60} \times 3$ $TiCl_4$).[15]

Spectroscopic characterization

In addition to the X-ray diffraction experiments, the title compound was characterized by vibrational spectroscopy. Fourier-transform infrared (FT-IR) spectroscopy predominately shows an intense $\nu(Ti–Cl)$ vibration at 486 cm^{-1} (Fig. 4a), which is very similar in wavelength and intensity to that observed in $TiCl_4$.[16] Moreover, broad less characteristic bands occur at
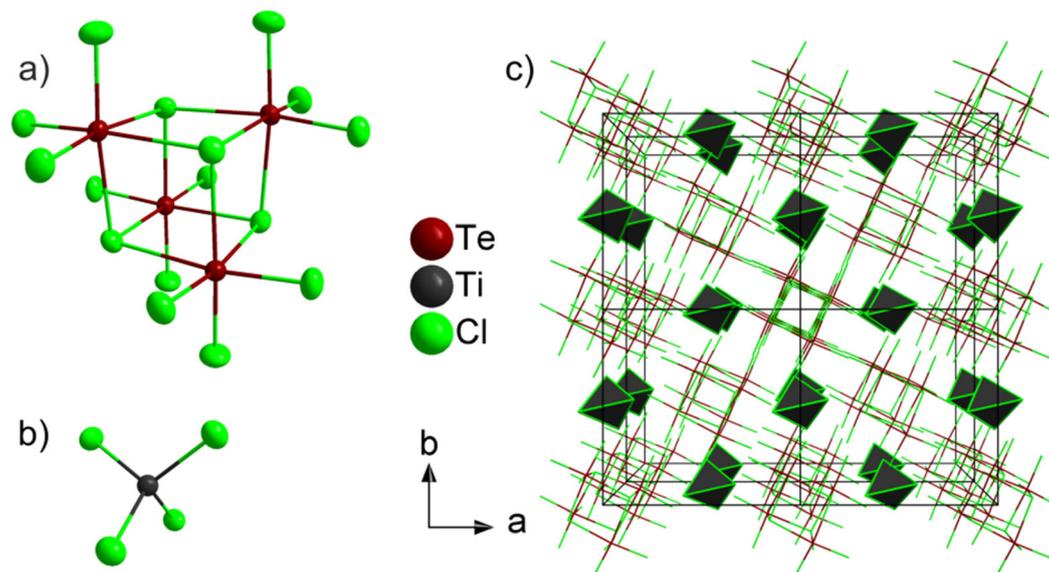
Fig. 3 Crystal structure of $(TeCl_4)_4(TiCl_4)$: (a) isolated $(TeCl_4)_4$ heterocubane, (b) isolated $TiCl_4$ tetrahedron; (c) (2 × 2 × 2) supercell showing the identical orientation of all $TiCl_4$ tetrahedra and $(TeCl_4)_4$ heterocubanes.
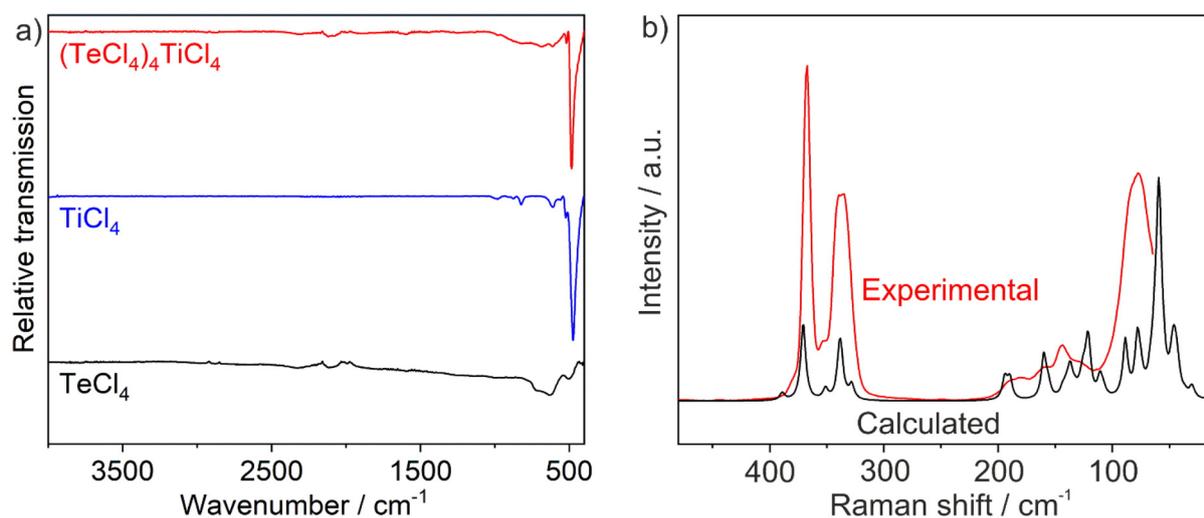

Fig. 4 Vibrational spectroscopy of $(TeCl_4)_4(TiCl_4)$: (a) FT-IR spectra (with $TeCl_4$ and $TiCl_4$ as references), (b) experimental and calculated Raman spectrum.

1000–500 cm^{-1} and are mainly due to motions of $TeCl_4$.[17] The absence of ν(O–H) or ν(C–H) vibrations at 3500–2800 cm^{-1} confirms the purity of the title compound, which is especially important due to its high moisture-sensitivity. Raman spectra were also recorded (Fig. 4b). Here, the characteristic Raman vibrations of $TeCl_4$ and $TiCl_4$ were observed at 300–400 cm^{-1} and below 200 cm^{-1}.[18] DFPT calculations allow to determine the Eigen-vectors associated with the Raman bands (see ESI†). The two intense bands at 325 and 356 cm^{-1} are due to an asymmetric and a symmetric stretching vibration of the $TeCl_3$ groups. Eigen-vectors of the low frequency bands involve motions of all constituents and cannot be easily classified.

The optical properties of $(TeCl_4)_4(TiCl_4)$ were analysed by UV-Vis spectroscopy (Fig. 5a). The title compound shows a strong absorption at 300–450 nm, which can be assigned to a valence-band to conduction-band transition. This absorption causes the pale yellow colour of crystals of the title compound. Using a Tauc plot, an indirect band gap of 2.8 eV was determined (Fig. 5b). Finally, the thermal properties of $(TeCl_4)_4(TiCl_4)$ were examined *via* thermogravimetry (ESI: Fig. S3†). Accordingly, $(TeCl_4)_4(TiCl_4)$ quantitatively decomposes into the binary compounds $TiCl_4$ (sublimation at 100–150 °C) and $TeCl_4$ (sublimation at 200–400 °C).

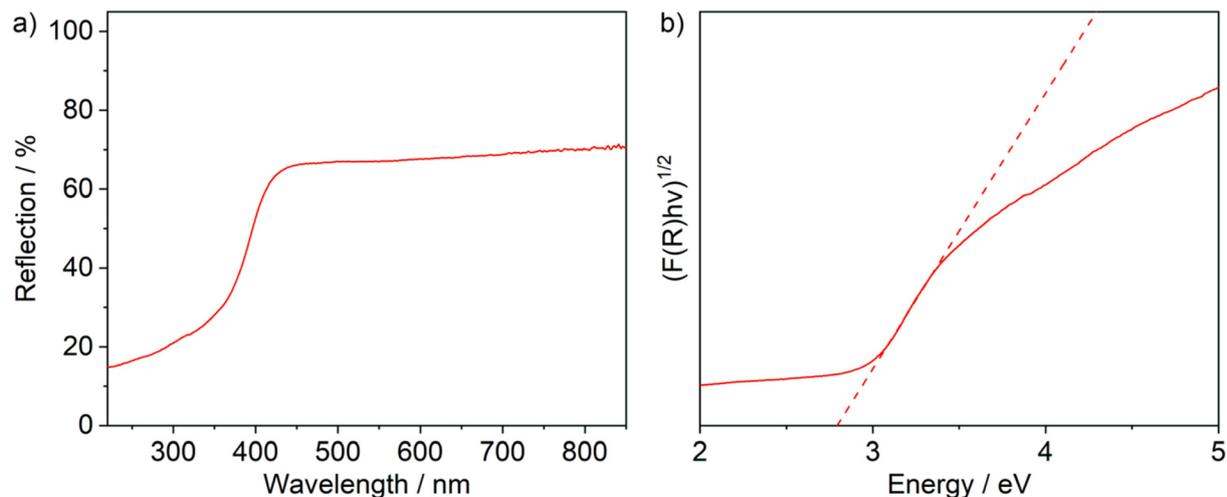**Fig. 5** Optical properties of $(TeCl_4)_4(TiCl_4)$: (a) UV-Vis spectrum, (b) Tauc plot.

Second harmonic generation

As $(TeCl_4)_4(TiCl_4)$ crystallizes in the non-centrosymmetric space group $I\bar{4}$, NLO effects such as SHG are to be expected, in principle.[1,19] The NLO behaviour of the title compound was therefore examined with the Kurtz–Perry method.[20] This method is well-suited for rapid characterization of new compounds as the analysis can be performed with microcrystalline powders. With crystallite sizes of 20 to 60 μm, moreover, the individual domains are large enough (>1 μm) to examine enantiomeric or twinned crystals. Due to the relationship between SHG intensity and grain size, the Kurtz–Perry method allows, in principle, to distinguish matchable and non-phase match-able materials. However, the averaged effective SHG coefficient derived from the experiment is associated with a large uncertainty as the grain-size distribution in a powder is difficult to quantify in moisture-sensitive materials, which cannot easily be sieved. Here, we used unsorted powder samples with grain sizes less than 25 μm, which were exposed to laser light at 1064 nm. The converted light was detected at 532 nm with the SHG intensities shown in Table 1.

As the Kurtz–Perry method does not result in absolute SHG intensities,[20] the reference compounds quartz and KDP were examined under similar conditions. KDP is phase matchable (second-order susceptibility: $d_{36} = 0.39$ pm V^{-1}) and can yield a SHG signal 5–10-times stronger than that of quartz ($d_{11} = 0.3$ pm V^{-1}), which is non-phase-matchable, under optimal

Table 1 SHG intensities of $(TeCl_4)_4(TiCl_4)$ and specific reference samples

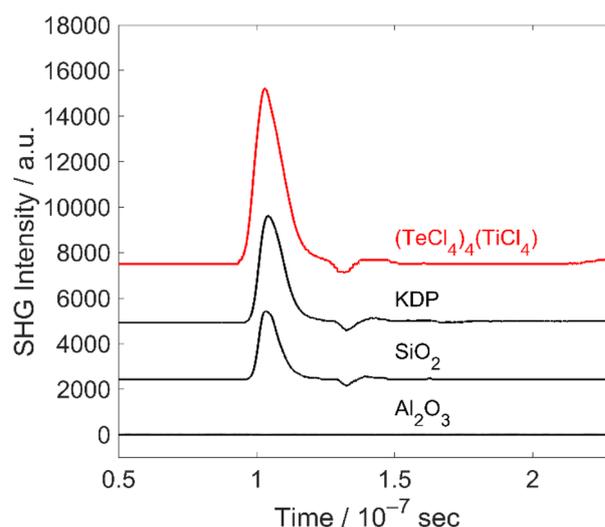| Sample	Particle size (μm)	SHG intensities (mV)
Al_2O_3	9	0 (1)
Quartz	<5	1632 (248)
	5–25	3552 (407)
KDP	5–25	5528 (822)
KDP	25–50	8860 (1067)
$(TeCl_4)_4(TiCl_4)$	<25	8632 (1104)

Fig. 6 Representative SHG measurements of $(TeCl_4)_4(TiCl_4)$ and reference samples (quantitative assessment not possible due to limitations of the Kurtz–Perry approach).

measurement conditions.[21] In our experiments, however, we had to use a focused laser and could only sample a few small selected spots. Due to this approach, the intensity difference between the two reference samples is significantly reduced. In addition, corundum (α-Al_2O_3) was analysed as a reference with inversion symmetry and, thus, not showing any SHG effect. In comparison, finally, $(TeCl_4)_4(TiCl_4)$ shows a significant SHG signal, which is about 1.6-times higher than that of KDP (Table 1, Fig. 6).

Conclusions

Aiming at Lewis acid–base reactions to obtain novel compounds with tetrahedral arrangements without inversion sym-

metry to establish second harmonic generation (SHG), we have reacted $TeCl_4$ and $TiCl_4$ at 50 °C. Against our expectation, no Lewis acid–base reaction to a compound like $[TeCl_3]^+[TiCl_5]^-$ or $[TeCl_3]_2^+[TiCl_6]^{2-}$ occurred. Instead, $(TeCl_4)_4(TiCl_4)$ was obtained with quantitative yield, which contains isolated, molecular $(TeCl_4)_4$ heterocubane-type units and isolated, molecular $TiCl_4$ tetrahedra. Such molecular building units – isolated $(TeCl_4)_4$ tetramers and molecular $TiCl_4$ tetrahedra – were rarely observed until now.

$(TeCl_4)_4(TiCl_4)$ crystallizes in the non-centrosymmetric space group $I\bar{4}$ with $(TeCl_4)_4$ heterocubanes arranged like in a body-centred cubic cell and with $TiCl_4$ tetrahedra in 4 of the 6 octahedral sites. In accordance with the unidirectional alignment of the tetrahedral building units, $(TeCl_4)_4(TiCl_4)$ shows a good SHG intensity, which is even 1.6-times stronger than for potassium dihydrogen phosphate (KDP). The SHG effect determined via the Kurtz–Perry method is observed in the visible spectral regime of a narrow-band-gap compound (E_g: 2.8 eV). The compound shows that tetrahedral arrangements with non-linear optic (NLO) effects can be easily obtained in quantitative yield with simple reactions near room temperature (≤100 °C), which also offers many options for further reactions and compounds with promising optical properties.

Experimental section

General considerations

The starting materials $TeCl_4$ (99% Sigma-Aldrich, Germany) and $TiCl_4$ (99.9%, Sigma-Aldrich) were commercially available and used as received. All reactants were filled and stored in argon-filled glove-boxes (MBraun Unilab, Germany, O_2/H_2O < 1 ppm). The reactions were performed using standard Schlenk techniques and glass ampoules. All glass ware was evacuated three times to $<10^{-3}$ mbar, heated, and flushed with argon to remove all moisture.

$(TeCl_4)_4(TiCl_4)$

50 mg (0.19 mmol) of tellurium(IV) chloride and 102 μL (176.0 mg, 0.93 mmol) of titanium(IV) chloride were reacted under argon in a glass ampoule at 50 °C for one week. After cooling to room temperature with a rate of 1 K h^{-1}, pale yellow crystals of $(TeCl_4)_4(TiCl_4)$ were obtained with quantitative yield.

X-ray data collection and structure solution

Selected single crystals of $(TeCl_4)_4(TiCl_4)$ were covered with inert oil (perfluorpolyalkylether, ABCR, Germany) and deposited on a microgripper (MiTeGen, USA). Data collection was performed at 213 K on an IPDS II image plate diffractometer (Stoe, Germany) using Mo-K_α radiation (λ = 71.073 pm, graphite monochromator). Data reduction and absorption correction were performed by the X-AREA software package (version 1.75, Stoe) and Stoe LANA (Version 1.63.1, Stoe).[22] For structure solution and refinement, SHELXT and SHELXL were used.[23] All atomic displacement parameters were refined anisotropically. Images were generated with DIAMOND.[24] Further details

related to the crystal structure may also be obtained from the joint CCDC/FIZ Karlsruhe deposition service on quoting the CSD-no. 2328371.

Second harmonic generation

Second harmonic generation (SHG) measurements were performed using the Kurtz–Perry approach[20] on microcrystalline powder samples clamped between two glass slides in order to avoid any exposure to air. Quartz, Al_2O_3 and KH_2PO_4 (KDP) were used as reference materials. A Q-switched Nd:YAG laser (1064 nm, 5–6 ns, 2 kHz) was used for the generation of the fundamental pump wave. The fundamental infrared light was focused into the sample and the generated second harmonic (532 nm) was separated from 1064 nm using a harmonic separator, a short-pass filter, and an interference filter. The SHG signal was collected with a photomultiplier and an oscilloscope from eight different areas of the sample. On each position, 64 pulses were measured and averaged. Background signals between the laser pulses were used to correct the measured intensities. The SHG measurements were performed under ambient conditions in transmission geometry.

Raman spectroscopy

Raman measurements were carried out with a custom set-up in Frankfurt described in detail elsewhere.[17] We used an OXXIUS S.A. Laser-Boxx LMX532 laser (λ = 532 nm) and a spectrograph (Princeton Instruments ACTON SpectraPro 2300i) equipped with a Pixis256E CCD camera. Measurements were performed in reflection geometry with the polarized laser light on the samples which were used for SHG measurements.

Conflicts of interest

There are no conflicts to declare.

Acknowledgements

References

1 E. Garmire, *Opt. Express*, 2013, **21**, 30532–30544.
2 C. J. Winta, S. Gewinner, W. Schöllkopf, M. Wolf and A. Paarmann, *Phys. Rev. B*, 2018, **97**, 094108.
3 R. W. Boyd, *Nonlinear Optics*, Academic Press, New York, 4th edn, 2020.
4 M. Jia, X. Cheng, M.-H. Whangbo, M. Hong and S. Deng, *RSC Adv.*, 2020, **10**, 26479.

5 (*a*) J. Chen, C. L. Hu, F. Kong and J. G. Mao, *Acc. Chem. Res.*, 2021, **54**, 2775–2783; (*b*) S. Shi, C. Lin, G. Yang, L. Cao, B. Li, T. Yan, M. Luo and N. Ye, *Chem. Mater.*, 2020, **32**, 7958–7964; (*c*) J. Y. Chung, H. Jo, S. Yeon, H. R. Byun, T.-S. You, J. I. Jang and K. M. Ok, *Chem. Mater.*, 2020, **32**, 7318–7326; (*d*) M.-L. Liang, Y.-X. Ma, C.-L. Hu, F. Kong and J.-G. Mao, *Chem. Mater.*, 2020, **32**, 9688–9695.

6 P. S. Halasyamani and W. Zhang, *Inorg. Chem.*, 2017, **56**, 12077–12085.

7 (*a*) B. A. Stork-Blaisse and C. Romers, *Acta Crystallogr., Sect. B: Struct. Crystallogr. Cryst. Chem.*, 1971, **27**, 386–392; (*b*) V. B. Rybakov, L. A. Aslanov, S. V. Volkov, Z. A. Fokina and N. I. Timoshchenko, *Zh. Neorg. Khim.*, 1991, **36**, 2541–2548.

8 (*a*) B. Neumüller, C. Lau and K. Dehnicke, *Z. Anorg. Allg. Chem.*, 1996, **622**, 1847–1853; (*b*) J. Beck and T. Schlörb, *Z. Kristallogr.*, 1999, **214**, 780–785.

9 M. A. Bonnin, L. Bayarjargal, V. Milman, B. Winkler and C. Feldmann, *Inorg. Chem. Front.*, 2023, **10**, 2636–2644.

10 M. A. Bonnin, L. Bayarjargal, S. Wolf, V. Milman, B. Winkler and C. Feldmann, *Inorg. Chem.*, 2021, **60**, 15653–15658.

11 (*a*) J. Wernet, *Z. Anorg. Allg. Chem.*, 1953, **272**, 279–287; (*b*) E. Wendling and J. De Lavillandre, *Bull. Soc. Chim. Fr.*, 1967, 2142–2148.

12 B. Buss and B. Krebs, *Inorg. Chem.*, 1971, **10**, 2795–2800.

13 A. Dawson, A. Parkin, S. Parsons, C. R. Pilham and A. L. C. Young, *Acta Crystallogr., Sect. E: Struct. Rep. Online*, 2002, **58**, i95–i97.

14 A. Y. Makarov, I. Y. Bagryanskaya, Y. M. Volkova, M. M. Shakirov and A. V. Zibarev, *Eur. J. Inorg. Chem.*, 2018, 1322–1332.

15 S. I. Troyanov and E. Kemnitz, *Russ. J. Inorg. Chem.*, 2001, **46**, 1547–1552.

16 N. J. Hawkins and D. R. Carpenter, *J. Chem. Phys.*, 1955, **23**, 1700–1702.

17 R. Ponsioen and D. J. Stufkens, *Recl. Trav. Chim. Pays-Bas*, 1971, **90**, 521–5287.

18 (*a*) J. E. Griffiths, *J. Chem. Phys.*, 1968, **49**, 642–647; (*b*) N. S. Gonçalves and L. K. Noda, *J. Mol. Struct.*, 2017, **1146**, 750–754; (*c*) A. Kovács and R. J. Konings, *J. Mol. Struct.*, 1997, **410–411**, 407–410.

19 H. D. Flack, *Helv. Chim. Acta*, 2003, **86**, 905–921.

20 S. Kurtz and T. Perry, *J. Appl. Phys.*, 1968, **39**, 3798–3813.

21 A. Ashkin, G. D. Boyd and D. A. Kleinman, *Appl. Phys. Lett.*, 1965, **6**, 179–180.

22 *X-RED, Data Reduction Program*, Stoe, Darmstadt, Germany, 2001.

23 G. M. Sheldrick, *Acta Crystallogr., Sect. A: Found. Adv.*, 2015, **71**, 3–8.

24 *DIAMOND, Crystal and Molecular Structure Visualization*, Crystal Impact GbR, Bonn, Germany, 2016.